MADRID
inter.noise 2019
June 16 - 19
NOISE CONTROL FOR A BETTER ENVIRONMENT

Frequency Responses of Acoustic Black Hole Wedges Solved by the Partition of Unity Finite Element Method

T. Zhou[1]
Department of Mechanical Engineering,
The Hong Kong Polytechnic University, Hong Kong, China

J.-D. Chazot[2]
E. Perrey-Debain[3]
Laboratoire Roberval, FRE CNRS,
Sorbonne Universités, Université de Technologie de Compiègne, France

L. Cheng[4,*]
Department of Mechanical Engineering,
The Hong Kong Polytechnic University, Hong Kong, China

ABSTRACT

The Acoustic Black Hole (ABH) phenomenon can be capitalized to manipulate and mitigate flexural waves in thin-walled structures. It features unique space-dependent wavenumber variation and wave celerity reduction in the tapered ABH area, thus posing great challenges to the existing modelling methods. In this work, the Partition of Unity Finite Element Method (PUFEM) is revamped to resolve the frequency response of an ABH beam. The method allows incorporating auxiliary interpolation functions in the finite element framework in order to better cope with the ABH oscillating behaviour. Several types of tapered Timoshenko beam elements are constructed by employing enrichment functions based on the ABH wave solutions with the WKB approximations (for general profiles) or the exact solutions (for parabolic profiles). Other enrichment bases, including polynomials, Fourier series and wavelets, are also investigated as hierarchic refinements. Using these enriched elements, structural responses of an ABH beam are computed and compared with the standard FEM. It is shown that the PUFEM can be easily adapted to model ABH effects with a good accuracy and efficiency, outperforming the conventional FEM for solving ABH problems.

Keywords: ABH, PUFEM, WKB method
I-INCE Classification of Subject Number: 42

[1] tong.fr.zhou@connect.polyu.hk
[2] jean-daniel.chazot@utc.fr
[3] emmanuel.perrey-debain@utc.fr
[4] li.cheng@polyu.edu.hk

1. INTRODUCTION

The Acoustic Black Hole (ABH) effect shows prospects for the manipulation and mitigation of the flexural waves in thin-walled structures. The ABH-featured structures consist of a tapered thickness profile which smoothly decreases according to a power-law profile [1]. As the incident flexural waves travel towards the indented ABH area, the wavenumbers increase continuously and the wave celerity reduces gradually alongside an amplification of the wave amplitude. In an ideal scenario when the thickness is tapered down to zero, waves will spend infinite time travelling inside the ABH beam, resulting in no wave reflections. Meanwhile, the vibrational energy is focalized and accumulated in the thin tapered region due to the wave modulations or compressions induced by the structural inhomogeneity. In practical cases where the zero thickness is non-achievable, applying surface damping treatment over the tapered region can significantly reduce the wave reflections and enhance the energy absorption [2]. ABH structures feature unique space-dependent wavenumber variation and wave celerity reduction. Therefore, most modelling methods require a refined discretization scheme with high resolution in order to capture the strong localized and highly oscillatory ABH behaviours [3-5]. This, however, leads to a drastic increase in the computational cost, which may become critical when dealing with more complicated ABH problems such as structures with multiple embedded and auxiliary ABH absorbers [6,7], parameter optimizations of ABH tapers [8,9], interactions of ABH structures with surrounding medium, and so on. Therefore, there is a need to develop more efficient methods to better tackle the ABH simulation problems.

In recent decades, enriched methods have been developed to offer improvements in the computational accuracy for short wave problems with lower computation efforts. These simulation techniques allow the incorporation of auxiliary functions with good approximation properties for the concerned problems in the formulation. As one of these enriched methods, the Partition of Unity Finite Element Method (PUFEM) [10,11] offers the advantages of sharing high similarities with conventional FEM, thus allowing easy implementation by using existing finite element meshes and codes [12,13]. In this work, the PUFEM is revamped to simulate the structural vibrations of an ABH beam. Different formulations are proposed to deal with the broadband ABH problems, seeking to improve the computational accuracy and efficiency of the PUFEM. Tapered Timoshenko beam elements are first constructed by employing various enrichment functions based on the ABH wave solutions with the WKB approximations (for general profiles) or the exact solutions (for parabolic profile). A “local” wave enrichment is studied for comparison purposes. Other enrichment bases, including polynomials, Fourier series and wavelets, are also investigated as hierarchic refinements. Using the built enriched elements, structural responses of an ABH wedge are computed and compared with the standard FEM.

2. FORMULATION

2.1 Problem Statement

Consider the flexural vibration of a beam with variable thickness. There are two main theories dedicated to beam: Euler-Bernoulli and Timoshenko theories. For the former, the axial displacement of the beam, at distance z from the neutral layer, is written as $u(x,z) = -zw_{,x}$, where $w(x,z) = w(x)$ is the lateral displacement of mid-

surface in z direction. For the latter, the beam axial displacements are replaced by $u(x,z) = z\beta(x)$, where $\beta(x)$ is the rotation angle of the cross section. The equation of motion of a tapered Euler-Bernoulli beam is given by

$$\left[EI(x)w_{,xx}\right]_{,xx} + \rho A(x)\ddot{w} - f_z = 0, \tag{1}$$

and the equations of motion of a tapered Timoshenko beams are

$$[\kappa GA(x)(\beta + w_{,x})]_{,x} - \rho A(x)\ddot{w} + f_z = 0, \tag{2}$$
$$\kappa GA(x)\left(\beta + w_{,x}\right) - [EI(x)\beta_{,x}]_{,x} + \rho I(x)\ddot{\beta} = 0, \tag{3}$$

where f_z is the distributed oscillating loading. The geometrical parameters are the moment of inertia I, the area of the cross-section A and the shear correlation factor κ. The material parameters are the Young's modulus E, the shear modulus G and the density ρ. The Euler-Bernoulli beam model, as a special case of Timoshenko beam, neglects the effects of shear deformation and rotary inertia. This simplified model is widely used in the literature to study the ABH phenomenon. Taking a simple supported beam as an example, the associated variational formulation for the tapered Timoshenko beam writes:

$$\int_0^L \left[w^*\rho A\ddot{w} + \beta^*\rho I\ddot{\beta} + \beta^*_{,x}EI\beta_{,x} + \left(\beta^* + w^*_{,x}\right)\kappa GA\left(\beta + w_{,x}\right) - w^* f_z\right]\mathrm{d}x - w_0^*\lambda_0 - w_L^*\lambda_L = 0, \tag{4}$$

where λ_0 and λ_L are Lagrange multipliers and L is the beam length. To handle the boundary terms with PUFEM, the essential boundary condition is enforced as:

$$\lambda_0^* w_0 = \lambda_L^* w_L = 0, \ \ \forall(\lambda_0^*, \lambda_L^*) \tag{5}$$

This approach also permits to handle the coupling conditions between two media with different wave speeds [14].

2.2 Wave Solutions

The closed-form solutions for Eq. 1 or Eqs. 2 and 3 in terms of elementary functions are difficult to be found. The analyses of these types of differential equations can be done approximately. The WKB method offers appropriate approximate solutions to the differential equations whose coefficients are slowly varying function in space [15]. For a tapered Euler-Bernoulli beam, the WKB solutions take the form

$$w(x,t) = \widehat{w}(\mathrm{x})e^{-i\omega t}e^{iS(x)}, \tag{6}$$

where $S(x)$ is the eikonal of the quasi-plane wave and $\widehat{w}(\mathrm{x})$ is the amplitude function. $S(x)$ can be found by integrating local wavenumber $k(x) = dS/dx$ over space. The local wavenumbers are expressed as

$$k(x) = \{\pm 1, \pm i\}[\omega^2\rho A(x)/EI(x)]^{1/4} \tag{7}$$

where the braces { , } donate the four possible values corresponding to the two travelling waves and two evanescent waves. The amplitude function $\widehat{w}(\mathrm{x})$ is determined

from the energy conservation law [1,15].The WKB solutions for the tapered Timoshenko beam write

$$\{w(x,t),\beta(x,t)\} = \{\widehat{w}(\mathrm{x}),\widehat{\beta}(\mathrm{x})\}e^{-i\omega t}e^{iS(x)}. \tag{9}$$

The local wavenumbers $k(x) = dS/dx$ corresponding to the four types of waves are given by

$$k(x) = \pm\left[\frac{1}{2}\left(\frac{1}{\kappa G}+\frac{1}{E}\right)\rho\omega^2 \pm \sqrt{\left(\frac{1}{\kappa G}-\frac{1}{E}\right)^2\rho^2\omega^4 + 4\frac{\rho A(x)}{EI(x)}\omega^2}\right]^2. \tag{9}$$

The displacement amplitude function is given in Ref. [15].

For a tapered Euler-Bernoulli beam with parabolic thickness variation $h(x) = \varepsilon x^2$, exact analytical solutions in terms of power functions can be derived [16]. The solution to Eq. 1 is sought by

$$w(x,t) = \widehat{w}e^{-i\omega t}x^v, \tag{10}$$

where

$$v = -\frac{3}{2} \pm \left[\frac{17}{4} \pm \sqrt{4+12\frac{\rho\omega^2}{E\varepsilon^2}}\right]^{1/2}. \tag{11}$$

Eq. 11 can be expressed in an exponential form.

2.3 Enriched Tapered Timoshenko Beam Elements

The PUFEM Timoshenko beam elements can be constructed by using different auxiliary enrichment functions. The lateral displacement and rotation are expanded, respectively, as:

$$w = \sum_{i=1}^{2} N_i(\eta) \sum_{n=1}^{N} A_{i,n}\Psi_{i,n}\,, \tag{12}$$

$$\beta = \sum_{i=1}^{2} N_i(\eta) \sum_{n=1}^{N} B_{i,n}\Phi_{i,n}\,. \tag{13}$$

Here, N_1 and N_2 are the shape functions of classical linear FEM and $\eta \in [-1,1]$ is the local coordinate. For the wave enrichment, the WBK approximate solutions for Euler-Bernoulli and Timoshenko beams and the exact analytical solutions for the Euler-Bernoulli beam can be taken as enrichment functions $\Psi_{\mathrm{i,n}}$ and $\Phi_{\mathrm{i,n}}$. A constant term is also added to the enrichment basis in order to capture the contribution of distributed loading. An enrichment based on "local" solutions for Eqs. 2 and 3 is also studied:

$$\{\Psi_{i,n}\,,\Phi_{i,n}\} \in \{1,\exp[k_{i,1}(x-x_i)]\,,\exp[k_{i,2}(x-x_i)]\,,\exp[k_{i,3}(x-x_i)]\,,\exp[k_{i,4}(x-x_i)]\} \tag{14}$$

where k_i are the local wavenumbers evaluated at the node x_i, using Eq. 9. Three other kinds of enrichment are also considered in this work.

Polynomial enrichment:

$$\{\Psi_{i,n}, \Phi_{i,n}\} \in \{1, \eta_i, \eta_i^2, \eta_i^3, \dots\}, \tag{15}$$

where $\eta_i = (x - x_i)/l_e$ (l_e is the length of the element).

Fourier-type enrichment:

$$\{\Psi_{i,n}, \Phi_{i,n}\} \in \{1, \cos \pi\eta_i, \sin \pi\eta_i, \cos 2\pi\eta_i, \sin 2\pi\eta_i, \dots\}, \tag{16}$$

Wavelet enrichment with the cardinal B-splines:

The cardinal B-splines, of order m, N_m, are used as scaling functions in the wavelet analysis. In this study the quantic B-spline with a scaling parameter $j \in \mathbf{Z}$ is chosen as the enrichment functions as:

$$\{\Psi_{i,n}, \Phi_{i,n}\} \in \{1, \dots, 2^{j/2} N_m(2^j \eta_i - n), \dots, \text{for } n \in \mathbf{Z}\}, \tag{17}$$

The wavelet functions have finite-support or fast-decaying oscillating shapes and possess superior approximating capability for the highly-localized ABH oscillating behaviour [5,17]. Other types of wavelets can also be chosen to replace cardinal B-splines.

3. NUMERICAL EXAMPLES

In this section, the Frequency Response Functions (FRF) are calculated by using different PUFEM elements and compared with the reference solutions offered by the classical linear FEM, obtained a sufficiently refined mesh (4000 elements). As a benchmark, a simply-supported tapered wedge (without an uniform portion) is considered in this paper. The geometrical and material parameters used in the simulations are given in Table 1. In a typical ABH structure, the tapered ABH area is usually non load-bearing due to the weakened stiffness. Therefore, loadings are usually applied at the uniform portion rather than the tapered portion. To eliminate the influence of contribution of distributed loading terms, i.e. the particular solution of the governing equations, on the evaluation of the performance of wave enrichment, the distributed loading used to activate the tapered wedge is chosen to have the same variation as the thickness profile.

Table 1. Parameters used in our computations

Wedge Thickness: $h(x) = 0.01(x + 0.02)^2/(0.2 + 0.02)^2$, $0 \le x \le 0.2$
Material Parameters (wedge): E=70 GPa , ρ=2780 kg/m^3 , G=27 GPa

Figures 1, 3, 4 and 5 show the FRF computed with PUFEM using different enrichment functions. The response location is at 1/4 of the beam length from the left end (x=0.05m). Figure 1 depicts the results using the wave enrichment based on WKB approximate solutions, using 16 elements with a same size (170 DoFs), and the exact analytical solutions. A good agreement between PUFEM and reference solutions can be

observed. The elements enriched with waves can provide accurate predictions within a broad and highly dynamic frequency band containing multiple structural resonances.

Figure 2 shows the structural response along the beam at the upper frequency limit of 40 kHz using Euler-Bernoulli WKB enrichment. One can observe the typical ABH phenomenon: the variation of local wavelengths and the increase of oscillation amplitudes due to the tailored structural thickness. The zoom-in sub-figure shows the detailed structural deformation within the 1st element on the left end (thinner part). One can see that one single enriched element can capture multiple wavelengths, which is typical of the wave enrichment, as well as the wave modulation effect.

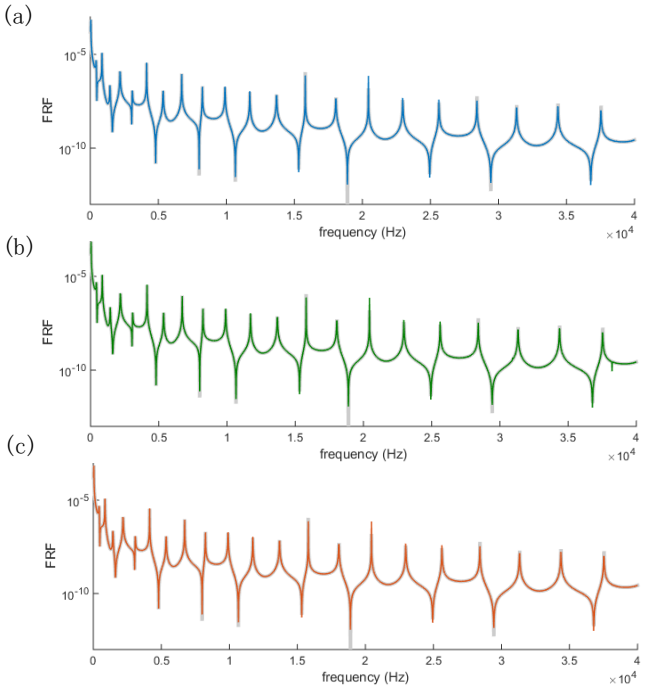

Figure 1. FRF using PUFEM (16 elements) with a) Euler-Bernoulli WBK enrichment (blue), b) Timoshenko WKB enrichment (green) and c) exact wave solutions (red) and reference solutions (grey).

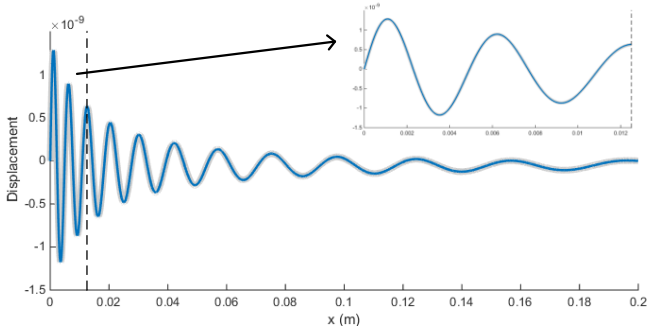

Figure 2. Wedge response at 40 kHz of PUFEM with Euler-Bernoulli WBK enrichment (blue) and reference solutions (grey). The subplot is the detailed response of the element at the left end).

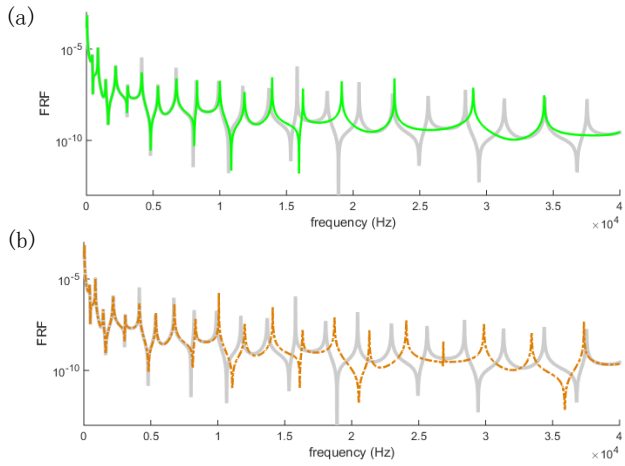

Figure 3. FRF of PUFEM (16 elements) with a) Euler-Bernoulli "local" wave enrichment (bright green), b) polynomial enrichment (dash-dot red) and reference solutions (grey).

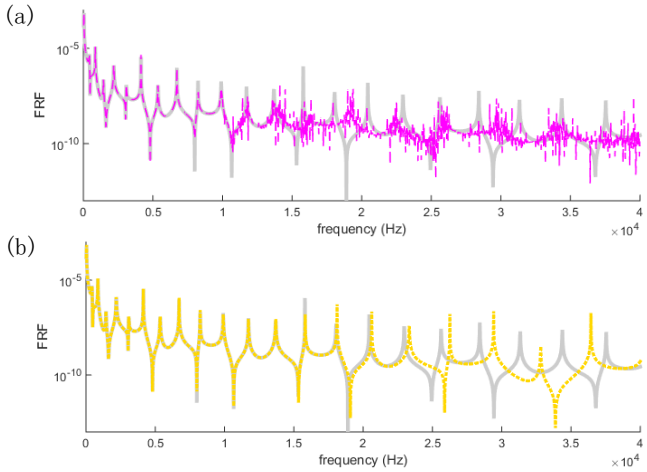

Figure 4. FRF of PUFEM (1 element) with a) Fourier enrichment (dash purple, 152 DoFs), b) wavelet enrichment (dot yellow, 172 DoFs) and reference solutions (grey).

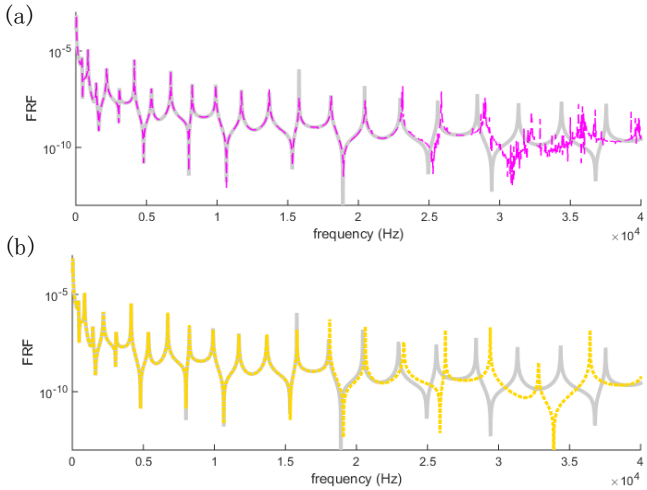

Figure 5. FRF of PUFEM (4 element) with a) Fourier enrichment (dash purple, 188 DoFs), b) wavelet enrichment (dot yellow, 170 DoFs) and reference solutions (grey).

In Figure 3, the FRF of the PUFEM with Euler-Bernoulli "local" wave enrichment and polynomial enrichment are computed using 16 elements (170 DoFs) and compared with the reference solutions. The "local" wave enrichment provides accurate results up to around 1.5 kHz, the polynomial enrichment can ensure the accuracy below

1kHz. The performance of the "local" wave enrichment is not as good as wave enrichment based on WKB or exact solutions. This is because the local wave solutions, which are only accurate in the vicinity of the nodes, can hardly represent the strong variation of wavenumbers and amplitudes within the element at higher frequencies.

The PUFEM with Fourier or wavelet enrichment should be better implemented by using an ordinary mesh with a high enrichment order N. This is due to the approximation properties of the enrichment functions. Figure 4 shows the FRF curves obtained from PUFEM simulation with Fourier and wavelet enrichment, using only 1 element and with similar DoFs as the wave enrichment used in Figure 1. The wavelet enrichment, with a scaling parameter j=4, is accurate up to 2.5 kHz and performs better than the Fourier enrichment. It was observed that the system matrix resulting from the Fourier enrichment becomes ill-conditioned above 1 kHz. This can be alleviated by increasing the element number and reducing the enrichment terms, as shown in Figure 5. The wavelet enrichment using scaling parameter j=3 (Figure 5) shows similar performance with the case of Figure 4. The element enriched with wavelets shows advantages over the one enriched with Fourier series. It also outperforms the elements enriched with "local" wave solutions and polynomials, but it is still not as good as the WKB enrichment.

4. CONCLUSIONS

In this work, tapered Timoshenko beam elements are developed to solve the forced response problem of an ABH wedge. Several types of enriched elements are constructed using different enrichment functions. The wave enrichment is based on WKB approximate solutions for general tapered Euler-Bernoulli and Timoshenko beams and exact analytical solutions for a parabolically tapered Euler-Bernoulli beam. Other types of enrichment are also considered in this work, including the "local" wave enrichment, polynomial enrichment, Fourier enrichment and wavelet enrichment. The performances of different enrichment are evaluated in terms of frequency response functions.

Through numerical explorations and comparisons with reference solutions, it was shown that the PUFEM is conducive to coping with ABH-related wave phenomena in a broad frequency band. Upon a proper selection of the enrichment scheme, accurate simulation could be achieved using a small number of elements or degrees of freedom. The capability of capturing multiple waves within an enriched element results in a significantly reduced computational cost.

The wave solutions with the WKB method are employed to build a FE- and wave-based model for ABH tapered structures. This formulation can also be employed for coping with other problems with spatially varying wave speeds. A new wavelet-based element is also developed for simulating structural vibrations. The PUFEM allows easy inter-element connection without scarifying the approximation properties of the wavelets. The enriched wavelet element also shows its versatility and flexibility as it could be used for other problems with quasi-singular solutions for instance. Our future works include applying the present numerical methods for solving other structural vibration problems.

5. ACKNOWLEDGEMENTS

The authors thank the support from Research Grant Council of the Hong Kong SAR (PolyU 152017/17E) and National Science Foundation of China (No. 11532006).

6. REFERENCES

[1] M. A. Mironov, *"Propagation of a flexural wave in a plate whose thickness decreases smoothly to zero in a finite interval,"* Sov. Phys. Acoust., vol. 34, no. 3, pp. 318–319, 1988.

[2] V. V Krylov and F. J. B. S. Tilman, *"Acoustic 'black holes' for flexural waves as effective vibration dampers,"* J. Sound Vib., vol. 274, no. 3, pp. 605–619, 2004.

[3] V. Denis, A. Pelat, F. Gautier, and B. Elie, *"Modal Overlap Factor of a beam with an acoustic black hole termination,"* J. Sound Vib., vol. 333, no. 12, pp. 2475–2488, 2014.

[4] T. Zhou, L. Tang, H. Ji, J. Qiu, and L. Cheng, *"Dynamic and static properties of double-layered compound acoustic black hole structures,"* Int. J. Appl. Mech., vol. 9, no. 05, p. 1750074, 2017.

[5] L. Tang, L. Cheng, H. Ji, and J. Qiu, *"Characterization of acoustic black hole effect using a one-dimensional fully-coupled and wavelet-decomposed semi-analytical model,"* J. Sound Vib., vol. 374, pp. 172–184, 2016.

[6] L. Tang and L. Cheng, *"Broadband locally resonant band gaps in periodic beam structures with embedded acoustic black holes,"* J. Appl. Phys., vol. 121, no. 19, p. 194901, 2017.

[7] T. Zhou and L. Cheng, *"A resonant beam damper tailored with Acoustic Black Hole features for broadband vibration reduction,"* J. Sound Vib., vol. 430, pp. 174–184, 2018.

[8] M. R. Shepherd, P. A. Feurtado, and S. C. Conlon, *"Multi-objective optimization of acoustic black hole vibration absorbers,"* J. Acoust. Soc. Am., vol. 140, no. 3, pp. EL227-EL230, 2016.

[9] C. A. McCormick and M. R. Shepherd, *"Optimal design and position of an embedded one-dimensional acoustic black hole,"* in 47th International Congress and Exposition on Noise Control Engineering, INTER-NOISE 2018.

[10] J. M. Melenk and I. Babuška, *"The partition of unity finite element method: Basic theory and applications,"* Comput. Methods Appl. Mech. Eng., vol. 139, no. 1, pp. 289–314, 1996.

[11] I. Babuška and J. M. Melenk, *"The Partition of Unity Method,"* Int. J. Numer. Methods Eng., vol. 40, no. 4, pp. 727–758, 1997.

[12] J.-D. Chazot, B. Nennig, and E. Perrey-Debain, *"Performances of the partition of unity finite element method for the analysis of two-dimensional interior sound fields with absorbing materials,"* J. Sound Vib., vol. 332, no. 8, pp. 1918–1929, 2013.

[13] J.-D. Chazot, E. Perrey-Debain, and B. Nennig, *"The partition of unity finite element method for the simulation of waves in air and poroelastic media,"* J. Acoust. Soc. Am., vol. 135, no. 2, pp. 724–733, 2014.

[14] O. Laghrouche, P. Bettess, E. Perrey-Debain, and J. Trevelyan, *"Wave interpolation finite elements for Helmholtz problems with jumps in the wave speed,"* Comput. Methods Appl. Mech. Eng., vol. 194, no. 2, pp. 367–381, 2005.

[15] A. D. Pierce, *"Physical interpretation of the WKB or eikonal approximation for waves and vibrations in inhomogeneous beams and plates,"* J. Acoust. Soc. Am.,

vol. 48, no. 1B, pp. 275–284, 1970.
[16] M. A. Mironov, *"Exact solutions of equation of transverse vibrations for a bar with a specific cross section variation law,"* Acoust. Phys., vol. 63, no. 1, pp. 1–6, 2017.
[17] L. Ma, S. Zhang, and L. Cheng, *"A 2D Daubechies wavelet model on the vibration of rectangular plates containing strip indentations with a parabolic thickness profile,"* J. Sound Vib., vol. 429, pp. 130–146, 2018.